Magnetization process of bilinear-biquadratic spin chains at finite temperature

Kouichi Okunishi
Department of Physics, Graduate School of Science, Osaka University, Toyonaka, Osaka 560-0043, Japan
(Received 19 February 1999)

We investigate magnetization process (M-H curve) of $S=1$ bilinear-biquadratic (BLBQ) spin chain near critical fields at finite temperatures. We use the density matrix renormalization group (DMRG) for the two-dimensional classical lattice model mapped by the Trotter decomposition, with a help of the Baxter's variational principle. By comparing the DMRG result of $S=1/2$ XY chain with the exact solution, we show that the DMRG is an efficient tool to calculate the M-H curve at finite temperatures. Further, we compute the M-H curve of the BLBQ chain. We compare the DMRG curve of the magnetization process of the BLBQ chain with those obtained by analytic approaches: correctly mapped δ-function Bose-gas approach and ''Bethe-ansatz approximation'' approach. Near the saturation field, we show that the δ-function Bose gas and the Bethe-ansatz approximation describe the M-H curve well in both at zero temperature and finite temperatures. Near the lower critical field, we find that the δ-function Bose gas is a good effective model at the Heisenberg point. We further find that the δ-function Bose gas cannot describe the M-H curve at finite temperatures, near the special point where the M-H curve changes qualitatively. [S0163-1829(99)02730-7]

I. INTRODUCTION

The magnetization process (M-H curves, where M is the magnetization and H is the applied field) of one-dimensional (1D) quantum spin chains has drawn much attention from the experimental and theoretical points of view. Magnetization measurements in high applied field, which have been developed rapidly, give clear evidence of the Haldane gap for NENP.[1] Recently the M-H curves for the bond-alternating spin chains were also investigated experimentally.[2] From theoretical viewpoint, it is important to investigate the M-H curve, because the M-H curve, reflecting the finite-H ground state, contains information about excited states at zero field. As for the $S=1$ bilinear-biquadratic (BLBQ) spin chain defined by the Hamiltonian

$$\mathcal{H}=\sum_i \left[S_iS_{i+1}+\beta(S_iS_{i+1})^2\right]-H\sum_i S_i^z, \qquad (1)$$

there have been few studies of the M-H curve away from the Heisenberg point ($\beta=0$). This is partially because the main interest in the BLBQ chain has been concentrated on the Haldane conjecture, and partially because numerical methods, for example, exact diagonalization and quantum Monte Carlo simulation,[3] have difficulty in investigating the M-H curves in the thermodynamic limit. At zero temperature, we have shown that product wave function renormalization group (PWFRG) method is an efficient tool to calculate the M-H curves.[4,5] The PWFRG method is a variant of the density matrix renormalization group (DMRG) method,[6] and is free from the convergency problem the original DMRG faces due to the sequence of level crossings in obtaining the M-H curve.

The DMRG has recently been developed also for a finite-temperature problem, where the system is mapped onto a 2D classical one via the Trotter-Suzuki transformation.[7,8] The DMRG in 2D classical lattice systems was developed by Nishino, where the symmetric transfer matrix is treated.[9] For the present problem, we have to deal with nonsymmetric transfer matrices. Then Baxter's variational principle, which was originally introduced by Kramers and Wannier, leads us to a smart extension of the DMRG to the nonsymmetric transfer matrix.[10–12]

Using this ''finite-temperature DMRG,'' we study in this paper the finite-temperature M-H curves of the BLBQ chain near the critical fields: $H_c=H_s$ for the saturation field and $H_c=\Delta$ for the lower critical field (Δ is the Haldane gap). In our previous work,[5] we have shown that the zero-temperature M-H curves near the critical fields can be described well by the δ-function Bose-gas (δ-BG) picture. In this picture, the H-M curve (not the M-H curve) is written by

$$|H-H_c|=\sigma\pi^2\Delta M^2\left(1+\frac{3}{\tilde{c}}\Delta M\right)+\mathcal{O}(\Delta M^4), \qquad (2)$$

where σ is inversely proportional to the boson mass, $\tilde{c}$ is the effective coupling constant of the δ-BG, and $\Delta M=1-M$ for $H_c=H_s$ or $\Delta M=M$ for $H=\Delta$. Near the saturation field, we have seen excellent agreement between the PWFRG calculated H-M curves and the δ-BG curves with the ''correct'' coupling constant $\tilde{c}$ obtained by the S-matrix approach.[5] Near the lower critical field, we have also shown that the H-M curves obtained by the PWFRG are consistent with the δ-BG prediction (2), except for a special point $\beta=\beta_c$ (≈ 0.41). Since the δ-BG is a low-energy effective model of the system, its validity may not be guaranteed at the finite temperatures where higher-energy modes of the system become non-negligible. Hence it is a very interesting problem to see to what extent the δ-BG can be applied to finite-temperature problems.

In the δ-BG treatment we have neglected lattice discreteness to put ''one-particle'' energy dispersion as $\varepsilon(k)=\sigma k^2$. For the finite-temperature problem, we must take account of the nonparabolicity of $\varepsilon(k)$ beyond the δ-BG, due to the

lattice discreteness. In this paper, we also discuss the Bethe-ansatz approximation (BAA) which is an extension of the low-energy effective S-matrix approach taken in the previous paper.[13,14]

This paper is organized as follows. In Sec. II, we explain the DMRG method for the 1D quantum system at finite temperatures. In Sec. III, we first check the reliability of the DMRG at the finite temperatures by comparing the exact solution of the XY spin chain. Next, we show the M-H curves of the BLBQ chain at various temperatures. In Sec. IV, we present the finite-temperature M-H curve obtained by the effective δ-BG approach and the BAA approach near the saturation field, and compare them with the DMRG results. In Sec. V, we compare the δ-BG prediction of the M-H curves near the lower critical field with the DMRG results. Finally, we give a summary in Sec. IV.

II. NUMERICAL RENORMALIZATION GROUP METHOD AT FINITE TEMPERATURE

By using the Trotter-Suzuki transformation, we can map the BLBQ chain to a 2D classical spin model, which can be treated by the transfer matrix method.[15] The transfer matrix, which is sometimes called quantum transfer matrix (QTM), is written as

$$T^{(N)} = T_1^{(N)} T_2^{(N)}, \tag{3}$$

where N means Trotter number. Each matrix element of $T_1^{(N)}$ and $T_2^{(N)}$ is given by

$$T_1^{(N)\{s\}}_{\{s'\}} = w(s_0,s_1|s_0',s_1')w(s_2,s_3|s_2',s_3')\cdots \times w(s_{N-2},s_{N-1}|s_{N-2}',s_{N-1}'), \tag{4}$$

$$T_2^{(N)\{s\}}_{\{s'\}} = w(s_1,s_2|s_1',s_2')w(s_3,s_4|s_3',s_4')\cdots \times w(s_{N-1},s_N|s_{N-1}',s_N'), \tag{5}$$

where $\{s\}$ and $\{s'\}$ denote spin configurations in a row, and $w(s_i,s_{i+1}|s_i',s_{i+1}')$ is a local Boltzmann weight. Because of the Trotter decomposition, we impose the periodic boundary condition $s_N = s_0$ and $s_N' = s_0'$. For the BLBQ chain the Boltzmann weight is given by

$$w(s_i,s_{i+1}|s_i',s_{i+1}') = \langle s_{i+1},s_{i+1}'|e^{-[S_iS_{i+1}+\beta(S_iS_{i+1})^2]/NT}|s_i,s_i'\rangle, \tag{6}$$

where T is temperature, and $\{|s_i,s_i'\rangle\}$ is the s^z diagonal basis for the site i and i'. In the QTM approach, thermodynamic behaviors of the system are calculated from the largest eigenvalue $\Lambda_{\max}^{(N)}$ of $T^{(N)}$ and the corresponding eigenvector $|\Lambda_{\max}^{(N)}\rangle$ in the $N\to\infty$ limit.

As was shown by Nishino, the DMRG can be applied to the transfer matrix in 2D classical lattice. In applying the DMRG to the present problem, we should note that our QTM $T^{(N)}$ is nonsymmetric, which needs an extension of the original implementation. For this purpose, it is helpful to recall the relation between the DMRG and the Baxter's corner transfer matrix (CTM) algorithm, which can solve the system with a nonsymmetric transfer matrix. Baxter's algorithm is based on the variational principle which dates back to the Kramers-Wannier work. This variational principle and the fact that the density matrix in the DMRG corresponds to a product of four CTMs lead us naturally to the DMRG for nonsymmetric transfer matrix, which is described as follows.

The method used in this paper is basically the finite-size algorithm of the DMRG.[6] We pick up a site n and decompose the transfer matrices into three parts. We then write each element as follows:

$$\mathcal{T}_1^{(N)i',j',\{s'\}}_{i,j,\{s\}} = P^l_{i',i}(s_0,s_{n-1}|s_0',s_{n-1}')w(s_{n-1},s_n|s_{n-1}',s_n') \times P^r_{j',j}(s_{n+1},s_0|s_{n+1}',s_0'), \tag{7}$$

$$\mathcal{T}_2^{(N)i',j',\{s'\}}_{i,j,\{s\}} = Q^l_{i',i}(s_0,s_{n-1}|s_0',s_{n-1}')w(s_n,s_{n+1}|s_n',s_{n+1}') \times Q^r_{j',j}(s_{n+1},s_0|s_{n+1}',s_0'), \tag{8}$$

for $n=$ odd, and

$$\mathcal{T}_1^{(N)i',j',\{s'\}}_{i,j,\{s\}} = P^l_{i',i}(s_0,s_{n-1}|s_0',s_{n-1}')w(s_n,s_{n+1}|s_n',s_{n+1}') \times P^r_{j',j}(s_{n+1},s_0|s_{n+1}',s_0'), \tag{9}$$

$$\mathcal{T}_2^{(N)i',j',\{s'\}}_{i,j,\{s\}} = Q^l_{i',i}(s_1,s_{n-1}|s_0',s_{n-1}')w(s_{n-1},s_n|s_{n-1}',s_n') \times Q^r_{j',j}(s_{n+1},s_1|s_{n+1}',s_0'), \tag{10}$$

for $n=$ even. In Eqs. (7) and (8), s_{n-1}, s_n, s_{n+1} and s_0 are bare-spin indices appearing in Eqs. (4) and (5), and block-spin indices i, i', j, and j' represent the spin configurations $\{s_1,\ldots,s_{n-2}\}$, $\{s_1',\ldots,s_{n-2}'\}$, $\{s_{n+2},\ldots,s_{N-1}\}$, and $\{s_{n+2}',\ldots,s_{N-1}'\}$, respectively. Accordingly, each element of the left and right eigenvectors belonging to the largest eigenvalue of $\mathcal{T}_1\mathcal{T}_2$ can be written as

$$\psi^L_{i,j}(s_1,s_n) \quad \text{and} \quad \psi^R_{j,i}(s_n,s_1). \tag{11}$$

In the ordinary DMRG approach, ψ^L and ψ^R are calculated by the standard Lanzcos diagonalization of $\mathcal{T}_1\mathcal{T}_2$.[6,9] However, our implementation is slightly different from the original ones. We consider the two transfer matrices $\mathcal{T}_1$ and $\mathcal{T}_2$ separately. Further we put a recursion relation for the eigenvectors.[16,17] Then we can improve them gradually by using multiplications of the transfer matrices (power method) instead of the Lanczos diagonalization.

Here, we should note that the Boltzmann weight of the system of our concern has reflection symmetry in the real space direction:

$$w(s_i,s_{i+1}|s_i',s_{i+1}') = w(s_i',s_{i+1}'|s_i,s_{i+1}). \tag{12}$$

Thus we can see easily the *right* and *left* eigenvector of $\mathcal{T}_2\mathcal{T}_1$ are ψ^L and ψ^R, respectively.

Starting from the initial eigenvectors ψ^L and ψ^R, we can improve them by the power method,

$$\psi^L(s_n,s_0) \leftarrow [\mathcal{T}_1\mathcal{T}_2]^\alpha \psi^L(s_n,s_0), \tag{13}$$

$$\psi^R(s_n,s_0) \leftarrow [\mathcal{T}_2\mathcal{T}_1]^\alpha \psi^R(s_n,s_0), \tag{14}$$

where α is an integer representing the number of the multiplication of the transfer matrix. We adopt $2\leqslant\alpha\leqslant 20$ in the

present paper. A larger α is requested as the system approaches a critical point. Using the improved eigenvectors, we construct the ''nonsymmetric density matrix'' ρ^l and ρ^r as follows:[12,18]

$$\rho^l_{i,j}(s_n)=\sum_{k,s_0}\psi^L_{i,k}(s_0,s_n)\psi^R_{k,j}(s_n,s_0), \tag{15}$$

$$\rho^r_{i,j}(s_n)=\sum_{k,s_0}\psi^R_{i,k}(s_0,s_n)\psi^L_{k,j}(s_n,s_0), \tag{16}$$

where the density matrices are block diagonal with respect to s_n. We diagonalize the non-symmetric density matrices to have

$$\rho^l_{i,j}(s_n)=\sum_k U^l_{i,k}(s_n)\omega^l_k V^{l\dagger}_{k,j}(s_n), \tag{17}$$

$$\rho^r_{i,j}(s_n)=\sum_k V^r_{i,k}(s_n)\omega^r_k U^{r\dagger}_{k,j}(s_n), \tag{18}$$

where U^l, U^r, V^l, and V^r are transformation matrices and ω^l and ω^r are eigenvalues of ρ^l and ρ^r. We then retain the larger mth eigenvalues and the corresponding left and right eigenvectors. The renormalization process of the ''partial transfer matrices'' P^l, P^r, Q^l, and Q^r is written as follows:

$$P^r_{i',i}(s_n,s_0|s'_n,s'_0)=\sum_{s_{n+1},s'_{n+1},k,l}V^{r\dagger}_{i,k}(s_n)P^r_{k,l}(s_{n+1},s_0|s'_{n+1},s'_0)V^r_{l,i}(s'_n), \tag{19}$$

$$Q^r_{j',j}(s_n,s_0|s'_n,s'_0)=\sum_{s_{n+1},s'_{n+1},k,l}U^{r\dagger}_{j',k}(s_n)w(s_n,s_{n+1}|s'_n,s'_{n+1})\times Q^r_{k,l}(s_{n+1},s_0|s'_{n+1},s'_0)V^r_{l,j}(s'_n), \tag{20}$$

$$P^l_{i',i}(s_0,s_n|s'_0,s'_n)=\sum_{s_{n-1},s'_{n-1},k,l}V^{l\dagger}_{i',k}(s_n)w(s_{n-1},s_n|s'_{n-1},s'_n)\times P^l_{k,l}(s_0,s_{n-1}|s'_0,s'_{n-1})V^l_{l,i}(s'_n), \tag{21}$$

$$Q^l_{j',j}(s_0,s_n|s'_0,s'_n)=\sum_{s_{n-1},s'_{n-1},k,l}U^{l\dagger}_{j',k}(s_n)\times Q^l_{k,l}(s_0,s_{n-1}|s'_0,s'_{n-1})U^l_{l,j}(s'_n), \tag{22}$$

for $n=$ odd, and

$$P^r_{i',i}(s_n,s_0|s'_n,s'_0)=\sum_{s_{n+1},s'_{n+1},k,l}V^{r\dagger}_{i,k}(s_n)\times P^r_{k,l}(s_{n+1},s_0|s'_{n+1},s'_0)V^r_{l,i}(s'_n), \tag{23}$$

$$Q^r_{j',j}(s_n,s_0|s'_n,s'_0)=\sum_{s_{n+1},s'_{n+1},k,l}U^{r\dagger}_{j',k}(s_n)\times w(s_n,s_{n+1}|s'_n,s'_{n+1})\times Q^r_{k,l}(s_{n+1},s_0|s'_{n+1},s'_0)V^r_{l,j}(s'_n), \tag{24}$$

$$P^l_{i',i}(s_0,s_n|s'_0,s'_n)=\sum_{s_{n-1},s'_{n-1},k,l}V^{l\dagger}_{i',k}(s_n)\times w(s_{n-1},s_n|s'_{n-1},s'_n)\times P^l_{k,l}(s_0,s_{n-1}|s'_0,s'_{n-1})V^l_{l,i}(s'_n), \tag{25}$$

$$Q^l_{j',j}(s_0,s_n|s'_0,s'_n)=\sum_{s_{n-1},s'_{n-1},k,l}U^{l\dagger}_{j',k}(s_n)\times Q^l_{k,l}(s_0,s_{n-1}|s'_0,s'_{n-1})U^l_{l,j}(s'_n), \tag{26}$$

for $n=$ even. Clearly the renormalized partial transfer matrices are symmetric.

Due to the variational principle aspects of the DMRG, we should only obtain the ''fixed point'' matrices P^l, P^r, Q^l, and Q^r, and the ''fixed point'' vectors ψ^L and ψ^R, which satisfy the variational equation. To calculate ψ^L and ψ^R as the fixed point of the DMRG iterations, we do not need ''exact'' ψ^L and ψ^R at *each* DMRG iteration. Accordingly it is permitted for us to adopt small α in Eqs. (13) and (14). As a compensation of the sloppy evaluation of ψ^L and ψ^R, we must introduce recursion relations for the eigenvectors. For this purpose, we notice the fact that the matrices U and V have a physical meaning as ''translation operators,''[16,17,19] which leads us to

$$\psi^L_{\mathrm{new}i,j}(s_0,s_{n+1})=\sum_{s_n,k,l}V^{l\dagger}_{i,k}(s_n,s_0)\times\psi^L_{\mathrm{old}k,l}(s_0,s_n)V^{r\dagger}_{l,j}(s_{n+1},s_0), \tag{27}$$

$$\psi^L_{\mathrm{new}i,j}(s_0,s_{n-1})=\sum_{s_n,k,l}V^l_{i,k}(s_{n-1},s_0)\psi^L_{\mathrm{old}k,l}(s_0,s_n)V^r_{l,j}(s_n,s_0), \tag{28}$$

$$\psi^R_{\mathrm{new}i,j}(s_0,s_{n+1}) = \sum_{s_n,k,l} U^r_{i,k}(s_{n+1},s_0)\psi^R_{\mathrm{old}k,l}(s_0,s_n)U^l_{l,j}(s_n,s_0), \tag{29}$$

$$\psi^R_{\mathrm{new}i,j}(s_0,s_{n-1}) = \sum_{s_n,k,l} U^{r\dagger}_{i,k}(s_n,s_0)\psi^R_{\mathrm{old}k,l}(s_0,s_n)U^{l\dagger}_{l,j}(s_{n-1},s_0). \tag{30}$$

For the infinite-size method, where U and V are uniform,[19] a similar recursion relation was successfully utilized to formulate the PWFRG method.[16] The recursion relations (27), (28), (29), and (30) are essentially identical to the ones used in the acceleration algorithm of the finite-size DMRG for 1D quantum systems.[17]

In the following sections, we apply the above method to calculations of the M-H curves of 1D quantum spin chains at finite T.

III. NUMERICAL RESULTS

A. XY model

We apply the DMRG described in the previous section to the $S=1/2$ XY spin chain in magnetic fields, to check the validity of the method for the calculation of the M-H curve. We should note that the magnetized state is generally gapless at zero temperature. Hence the efficiency of the DMRG is not trivial at low temperatures. The Hamiltonian of the XY chain is given by

$$\mathcal{H}=\sum_i (S^x_i S^x_{i+1}+S^y_i S^y_{i+1})-H\sum_i S^z_i. \tag{31}$$

This model is soluble via Jordan-Wigner transformation; the M-H curve at finite temperature T is known to be[20,21]

$$M=\frac{1}{2\pi}\int_{-\pi}^{\pi}\tanh\left(\frac{\cos k+H}{2T}\right)dk. \tag{32}$$

In Fig. 1, we compare the numerical results to the exact curve (32). We can see excellent agreement. The DMRG calculation is done with only $m=16$. As for the Trotter number dependence of M, we have obtained a converged result within $N=28$ even at the lowest temperature $T=0.1$. We have thus confirmed the efficiency of the DMRG for the M-H curve of the $S=1/2$ XY spin chains.

B. BLBQ chain

In Fig. 2, we show the M-H curves of the BLBQ chain for $\beta=0$ (Heisenberg point), 1/3 (AKLT point[22]), and 0.6 at $T=0.1$, 0.2, and 0.5. The maximum Trotter number and the retained bases used in the present calculations are as follows: $N=36$ and $m=30$ for $T=0.1$, and $N=20$ and $m=27$ for $T=0.2$, and 0.5. We have confirmed that, with these N and M, the magnetization is converged within the order of 10^{-4}.

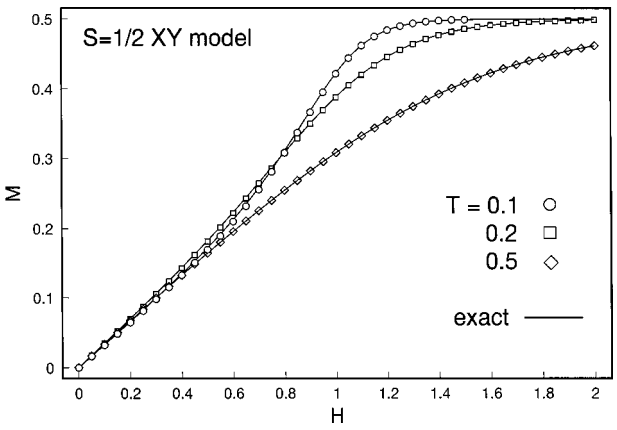

FIG. 1. Comparison of the DMRG result and the exact solution of the $S=1/2$ XY model for $T=0.1$, 0.2, and 0.5. We can see excellent agreement.

As we have announced in the previous paper,[5] the M-H curve for $\beta=0.6$ at $T=0$ has a cusp at $H\simeq 1.0$. We can see that the cusp is rounded by the finite-temperature effect.

IV. NEAR THE SATURATION FIELD

A. δ-function Bose-gas model

Let us consider the system near the saturation field ($H_s=4$), where the low-energy properties are well described by the effective δ-BG picture.[5,23,24] Above the saturation field, the ground state is the fully polarized (''all up'' state) spin, and each ''0'' spin is regarded as an elementary excitation. As the applied field H decreases below H_s, the number of the ''0'' spins increases, and the interaction between them becomes to be non-negligible (see Fig. 3). Taking the interaction effect into account, we may describe the system near the saturation field by the effective δ-BG model, whose Hamiltonian is given by

$$\mathcal{H}_{BG}=\int dx[\partial_x\phi^\dagger(x)\partial_x\phi(x)+c\,\phi(x)\phi^\dagger(x)\phi^\dagger(x)\phi(x)], \tag{33}$$

where $\phi(x)$ is the boson-field operator and c is the coupling constant. The external field H corresponds to the chemical potential, and the magnetization per site M is expressed as $M=1-\int dx\langle\phi^\dagger(x)\phi(x)\rangle$.

The BLBQ chain on the lattice can be related with the δ-BG model in terms of the S matrix of two down spins. The key idea is that, in the low-energy limit, the two-body S matrix reduces to that of the δ-BG model.[5] We denote the S^z-diagonal bases of the spin chain as $\{|\sigma_1,\sigma_2,\ldots,\sigma_N\rangle\}$, where σ_i $(=0,\pm 1)$ is the eigenvalue of the S^z operator at site i.

To solve the scattering problem of two down spins,

$$\mathcal{H}|\Psi\rangle=E^{(2)}|\Psi\rangle, \tag{34}$$

we put

$$|\Psi\rangle=\sum_{y>x}\psi(x,y)|\ldots,1,\underset{x}{0},1,\ldots,1,\underset{y}{0},1,\ldots\rangle + \sum_z f(z)|\ldots,1,\underset{z}{-1},1,\ldots\rangle. \tag{35}$$

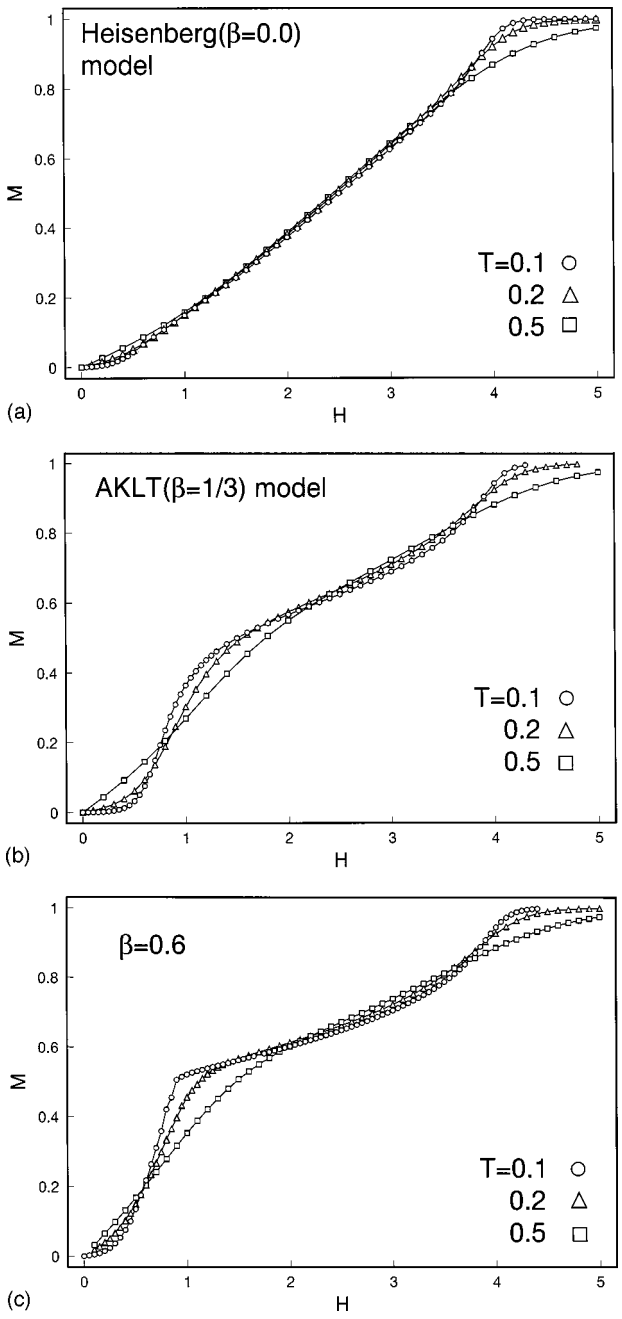

FIG. 2. The M-H curve of the BLBQ chain for $\beta=0,1/3,0.6$ and $T=0.1,0.2,0.5$: (a) $\beta=0$ ($S=1$ Heisenberg model), (b) $\beta=1/3$ (AKLT model), and (c) $\beta=0.6$.

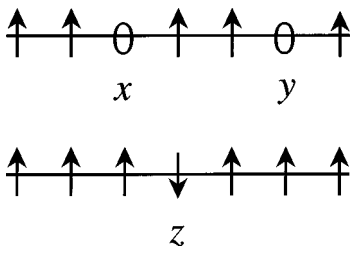

FIG. 3. Schematic diagram of two-body problem near the saturation field. One ''0'' spin is regarded as an elementary excitation in the fully polarized (ferromagnetic) state. We solve the two ''0'' spin problem exactly and obtain the effective S matrix.

The solution of the two-body problem is given as

$$\psi_{k,k'}(x,y)\sim e^{ikx}e^{ik'y}+S_{\mathrm{BAA}}(k,k')e^{ik'x}e^{iky}, \tag{36}$$

$$E^{(2)}(k,k')=E(k)+E(k'), \tag{37}$$

where $E(k)\equiv -2+2\cos k$ is the one-particle energy and $S_{\mathrm{BAA}}(k,k')$ is the exact two-body S matrix:

$$S_{\mathrm{BAA}}(k,k') =-\frac{3\beta+1-(\beta-1)\kappa\kappa'+i(\kappa-\kappa')[2\beta-(\beta-1)\kappa\kappa']}{3\beta+1-(\beta-1)\kappa\kappa'-i(\kappa-\kappa')[2\beta-(\beta-1)\kappa\kappa']}, \tag{38}$$

with $\kappa=\cot(k/2)$ and $\kappa'=\cot(k'/2)$.[14,25] Since the one down-spin energy takes its minimum at $k=\pi$, the low-energy scattering behavior is described by the ''effective S matrix'' given by making $k,k'\to\pi$ in Eq. (38). Explicitly, we have

$$S_{\mathrm{BAA}}(k,k') \overset{k,k'\to\pi}{\to} S_{\mathrm{BG}}(k,k')\equiv\frac{k-k'+ic}{k-k'-ic}, \tag{39}$$

where S_{BG} is the S matrix of the δ-BG with the coupling constant

$$c=-\frac{(3\beta+1)}{\beta}. \tag{40}$$

In the same limit, the one-particle energy dispersion curve becomes a parabola, which implies that the low-energy property of the BLBQ chain near H_s should be described by δ-BG with coupling $c=-(3\beta+1)/\beta$. Although this effective coupling constant is negative for $\beta>0$ or $\beta<-1/3$, the resulting δ-BG *without* bound states properly describes the system near the saturation field. In fact, at zero temperature, using the solution of the δ-BG obtained by Lieb and Liniger,[26] we can express the M-H curve near $H=H_c=H_s$ by Eq. (2) with $\sigma=1$ and $\tilde{c}=c$, which agrees very well with the PWFRG calculation.[5]

At finite temperatures, the thermal Bethe-ansatz method developed by Yang and Yang gives a set of integral equations,[27]

$$\varepsilon(k)=-\mu-k^2-\frac{Tc}{\pi}\int dp\frac{1}{c^2+(k-p)^2}\ln(1+e^{-\varepsilon(p)/T}), \tag{41}$$

$$\rho_{\mathrm{BG}}(k)(1+e^{\varepsilon(k)/T})=\frac{1}{2\pi}+\frac{c}{\pi}\int dp\frac{1}{c^2+(k-p)^2}\rho_{\mathrm{BG}}(p), \tag{42}$$

to determine the functions $\varepsilon(k)$ and $\rho_{\mathrm{BG}}(p)$ which describe various properties of the system. To obtain the M-H curve, we set the chemical potential in Eq. (41) to be $\mu=4-H$, and calculate the per-site magnetization M as

$$M=1-\int\rho_{\mathrm{BG}}(p)dp, \tag{43}$$

where ρ_{BG} (Bose-gas density distribution) is the solution of Eqs. (41) and (42).

B. Bethe-ansatz approximation

In the previous subsection, we have explained the effective δ-BG model that describes the spin chain correctly in the low-energy and low-density (=high-field) region. In this ''continuous'' Bose-gas mapping, we have put the one-particle energy dispersion to its low-energy limit, namely, a parabola, which is equivalent to neglecting the lattice discreteness. As a next stage of the approximation, we can employ the ''Bethe-ansatz approximation''[13,14] to take account of the lattice effect which may become relevant at finite temperatures. In the BAA, we apply the Bethe-ansatz method to a nonintegrable system, by *forcing* many-body scattering to be factorized into the two-body scattering. Clearly, the BAA automatically yields the exact result for the integrable cases $\beta=\pm 1$.[28,29] Further, even for nonintegrable cases, the BAA is exact within the two-body problem with full lattice discreteness; the lattice effect is properly taken into account. We can therefore expect the BAA to be good in the low particle density where many-body scattering is not dominant. In fact, for the BLBQ chain with $\beta\leqslant 0$, quite good agreement between the zero-temperature BAA and the exact diagonalization has been shown in Ref. 14. What we present in this subsection is a finite-temperature extension of the BAA.

In performing the finite-temperature BAA (''thermal BAA''), we simplify the analysis by neglecting the bound states, although they actually exist. Since the bound states for $\beta>-1/3$ are high-energy modes,[14] we can expect that the low-temperature behavior is not affected significantly by this simplification.

Following the standard BA method, we obtain

$$k_i N=2\pi I_i-i\sum_{j\neq i}\ln S_{\mathrm{BAA}}(k_i,k_j'), \tag{44}$$

where I_i is the quantum number (integer or half integer). Taking the thermodynamic limit ($N\rightarrow\infty$), Eq. (44) is converted to an integral equation. Making a variable change $k\rightarrow\tilde{k}=\cot(k/2)$ and rewriting $\tilde{k}$ to k for notational simplicity, we have an equation

$$f(k)=\frac{1}{1+k^2}-\int_{-B}^{B}K(p,k)f(p)dp, \tag{45}$$

where $f(k)$ is a density distribution and B is related to M. The explicit form of the kernel $K(k,p)$ is given by

$$K(k,p)=\frac{(\beta-1)^2k^2p^2+(\beta^2-1)p^2-2(3\beta+1)(\beta-1)kp+2\beta(3\beta+1)}{[3\beta+1-(\beta-1)kp]^2+(k-p)^2[2\beta-(\beta-1)kp]^2}. \tag{46}$$

Then the M-H curve at zero temperature is calculated from

$$M=1-\int_{-B}^{B}f(p)dp, \tag{47}$$

$$\epsilon(M)=\int_{-B}^{B}\frac{-4}{1+p^2}f(p)dp, \tag{48}$$

$$H-4=-\frac{\partial\epsilon(M)}{\partial M}. \tag{49}$$

In a similar fashion to the standard thermal BA within the ''one string'' (no bound state), we perform the thermal BAA, which gives a set of integral equations

$$\varepsilon(k)=H-\frac{4}{1+k^2}-\frac{T}{\pi}\int dpthK(p,k)\ln(1+e^{-\varepsilon(p)/T}), \tag{50}$$

$$\rho_{\mathrm{BAA}}(k)(1+e^{\varepsilon(k)/T})=\frac{1}{\pi(1+k^2)}-\frac{1}{\pi}\int dp\,K(k,p)\rho_{\mathrm{BAA}}(p). \tag{51}$$

The magnetization is then given by

$$M=1-\int\rho(k)dk. \tag{52}$$

C. Results and discussion

In the our previous paper,[5] we compared the zero-temperature M-H curve of the δ-BG model to the PWFRG calculation. The agreement is good in an unexpectedly wide

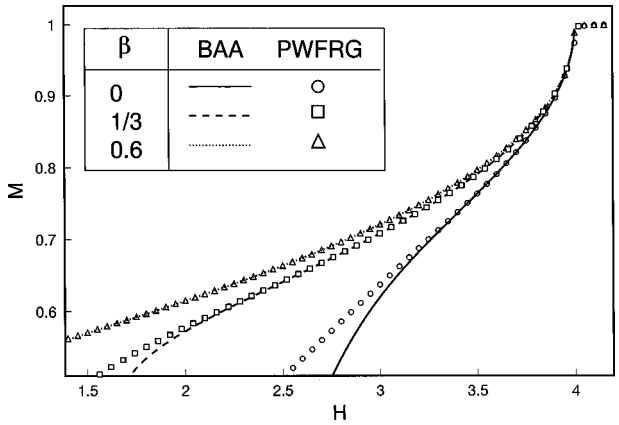

FIG. 4. The BAA result for $\beta=0$, 1/3, and 0.6 at the zero temperature. We are able to see the good agreement with the PWFRG results up to the middle region of the curve ($M>0.6$).

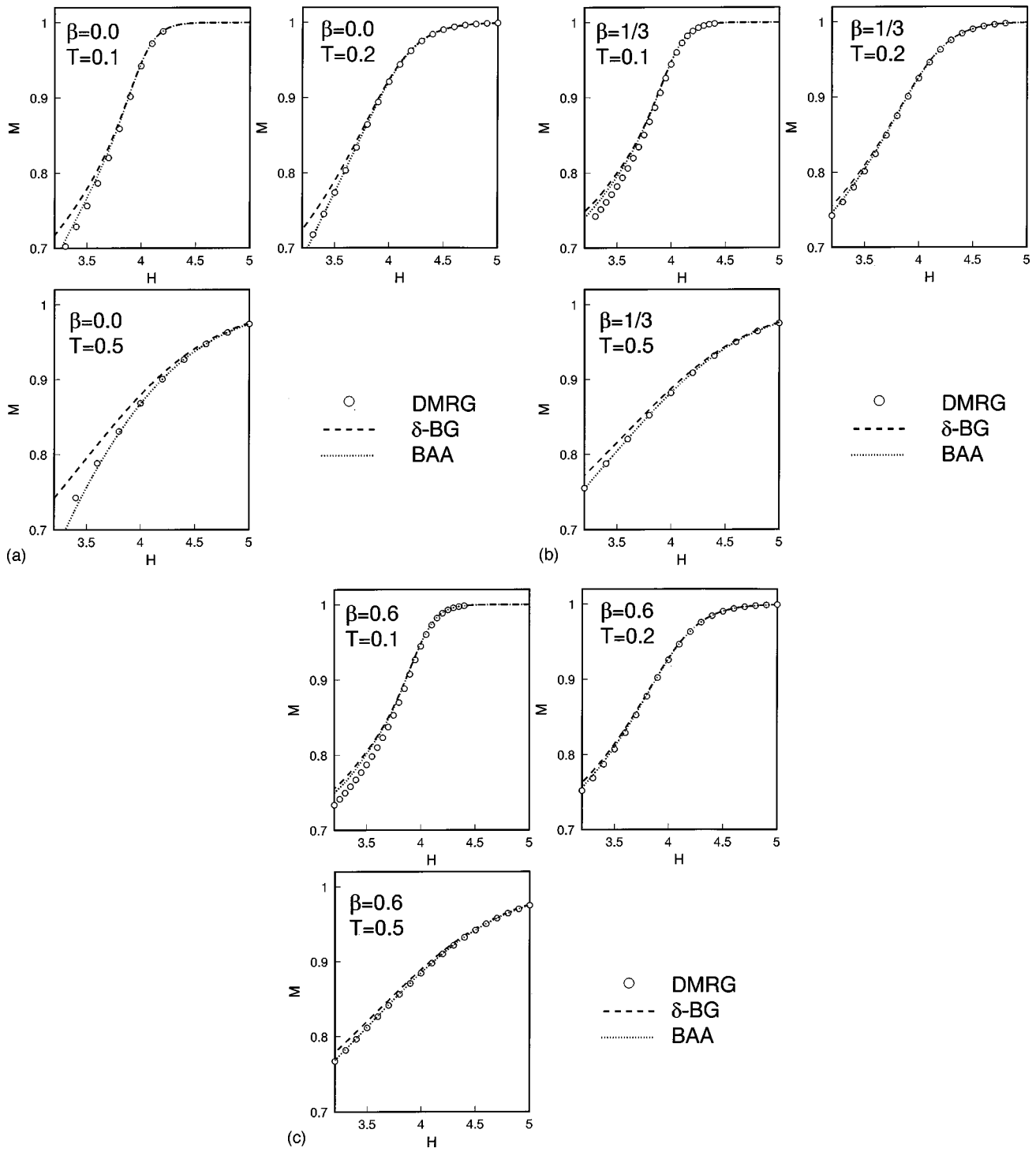

FIG. 5. The δ-BG and the BAA results near the saturation field at the finite temperatures: (a) $\beta=0$, (b) $\beta=1/3$, and (c) $\beta=0.6$.

region near the saturation field ($M>0.8$). In Fig. 4, we show a comparison of the present zero-temperature BAA results with the PWFRG results, where we see better agreement among them in a wider region of the M-H curve ($M>0.6$). We also find that as β approaches the integrable point $\beta=1$, the agreement becomes better and better. We thus have verified the validity of the BAA at the zero temperature.

In Fig. 5 we show the finite-temperature results. In the low-density region (i.e., high-field region with $M>0.95$), the DMRG results are reproduced very well by both the effective δ-BG approach and the BAA approach. In the middle field, the δ-BG curve begins to deviate significantly from the DMRG curve before $M=0.8$ (at zero temperature, the deviation is not so significant around this region.[5]) The DMRG results indicate that the shape of the M-H curves varies sensitively with temperature, while the δ-BG cannot reproduce such behaviors. On the other hand, the BAA curves agree with the DMRG curves even in the intermediate range of the field. The BAA approach, even without the bound state, successfully explains a considerable portion of the M-H curves

at finite temperatures. Further, we find that the BAA becomes better and better as β approaches the integrable point $\beta=1$.

Hence, we can conclude that the BAA is reliable not only at zero temperature but also at finite temperatures, in the wide region of the field near the saturation field.

V. NEAR THE LOWER CRITICAL FIELD

A. δ-function Bose gas model

Let us discuss the M-H curve near the lower critical field ($H_c=\Delta$). In this region, a microscopic derivation of an effective model is difficult, since the exact elementary excitation cannot be obtained analytically, unlike the case near the saturation field. We may then regard phenomenologically the triplet states above the singlet ground state as elementary excitations with the δ-function-type interactions. This picture was first given by Affleck and may be reasonable in terms of the Fermi-Luttinger liquid theory.[30]

Let us write the Hamiltonian of the effective δ-BG as

$$\mathcal{H}_{\mathrm{BG}}=\int dx\Bigg[\sigma\sum_{s}\partial_x\phi^{(s)\dagger}(x)\partial_x\phi^{(s)}(x)+\sum_{s,s'}c_{s,s'}\phi^{(s)\dagger}(x)\phi^{(s')\dagger}(x)\phi^{(s')}(x)\phi^{(s)}(x)\Bigg], \tag{53}$$

where s is an index of the S^z of the triplet excitation and takes $\{-1,0,1\}$. Although we do not have a direct mapping between the BLBQ Hamiltonian and Eq. (53), we can determine the parameters σ and c indirectly through the zero-temperature M-H curve; we make a fitting of the PWFRG calculation to the zero-temperature M-H curve deduced from Eq. (53). Then, calculating the finite-temperature M-H curve by using the resulting Hamiltonian (53), and comparing it with a finite-temperature DMRG result, we can check the validity of the Bose-gas mapping.

Further, we know that the low-energy excitations near the singlet ground state are given by the relativistic free fermion picture,[31] which was originally presented at the Heisenberg point. The one-particle dispersion curve near the bottom of the band ($k=\pi$) can be expressed as

$$\omega(k)=\sqrt{\Delta^2+v^2(k-\pi)^2}, \tag{54}$$

where v is called spin-wave velocity. Taking the low-energy limit $k\to\pi$, Eq. (54) becomes

$$\omega(k)=\Delta+\frac{v^2}{2\Delta}(k-\pi)^2. \tag{55}$$

Then, we get an equation

$$\sigma=\frac{v^2}{2\Delta}, \tag{56}$$

which relates the amplitude σ in the M-H curve with Δ and v in the low-energy dispersion curve. Hence it is also possible to check the consistency of the M-H curves with the values of v and Δ evaluated by other numerical computations.

TABLE I. Effective coupling constant $\tilde{c}$ and the inverse mass of the boson field σ estimated from the zero-temperature H-M curves.

β	0	1/3	0.6
$\tilde{c}$	0.37	0.83	-6.8
σ	7.6	0.49	0.70

In order to calculate the zero-temperature M-H curve from Eq. (53), we may omit $s=0,-1$ sectors (due to the Zeeman term).[24] Then the H-M curve is obtained as Eq. (2) with the amplitude σ and the effective coupling constant $\tilde{c}=c_{1,1}/\sigma$.[5] Comparison with the PWFRG calculations gives us the values of the parameters summarized in Table I.

At the finite temperatures, we should consider the other modes $\phi^{(0)}$ and $\phi^{(-1)}$. Although there may be nonzero interactions between the different modes, we assume that they are small to set the off-diagonal coupling constants $c_{s,s'}$ ($s\neq s'$) to be zero. As for the diagonal couplings, we put $c_{0,0}=c_{-1,-1}=c_{1,1}$ by symmetry. Replacing the parameters $c\to c/\sigma$, $\mu\to H$, and $k^2\to\sigma k^2$ in Eqs. (41) and (42), we obtain the M-H curve as

$$M=\int\rho_{\mathrm{BG}}^{(+1)}(k)dk-\int\rho_{\mathrm{BG}}^{(-1)}(k)dk, \tag{57}$$

where $\rho_{\mathrm{BG}}^{(+1)}(k)$ and $\rho_{\mathrm{BG}}^{(-1)}(k)$ are momentum-distribution functions (or the root-density functions in BA terminology) for the $s=\pm$ modes.

We should make a comment on the negative coupling constant which appears in $\beta>\beta_c$ (see Table I), because the naive attractive interaction makes the system unstable.[5] Recall that a physical picture of the excitations from the singlet ground state (Haldane state) is explained well in terms of the moving domain wall which separates two states with orientational order.[32–34] Since the number of domain walls which can occupy the same site cannot exceed the maximum local wall height ($=S$), the ''bound-state-forming instability'' caused by the negative coupling δ-BG may be avoided in the spin chain. However, the actual situation is more subtle, since the domain wall cannot be defined microscopically; the wall position itself is not so well defined because of the zero-spin defects destroying the positional order. We expect that the finite-temperature calculation gives us further information on nature of the excitations in the region $\beta_c<\beta<1$.

B. Results and discussion

In Fig. 6, we compare the δ-BG calculation with the DMRG results of the finite-temperature M-H curve.

For $\beta=0$, we can see quantitative agreement in the low fields ($M<0.1$). On raising the field, the δ-BG curves still keep qualitative agreement for all temperatures.

For $\beta=1/3$ (AKLT chain), the δ-BG curve of $T=0.2$ agrees with the DMRG result in very low fields. However, the curves of $T=0.1$ and $T=0.5$ do not agree with the DMRG results. The sensitive temperature dependence of the M-H curve obtained by the DMRG is not reproduced in the δ-BG curve. Use of the other value of σ, for example, $\sigma=0.5246\ldots$, which is the one in the dressed soliton approximation,[34] leads us to similar results. Let us recall that,

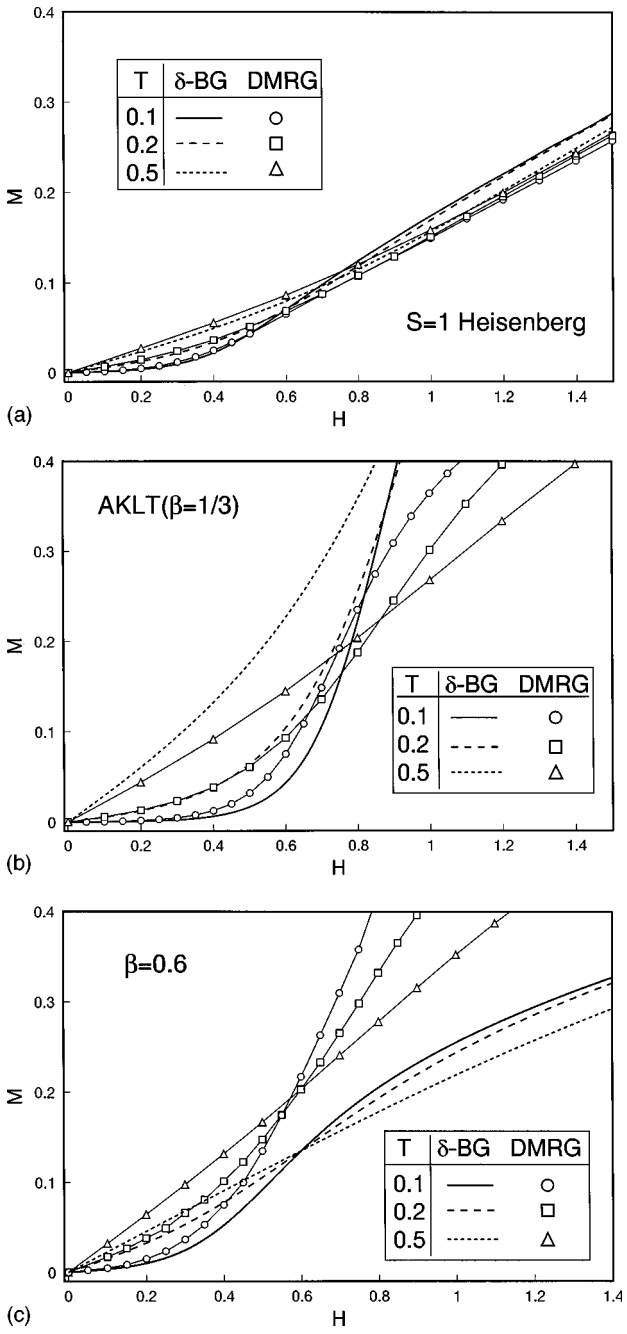

FIG. 6. The δ-BG results near the lower critical field: (a) $\beta=0$, (b) $\beta=1/3$, and (c) $\beta=0.6$.

at zero temperature, the M-H curve of the AKLT model rises more rapidly than that of $\beta=0$, implying that the region of H where the δ-BG picture is valid is narrow in the AKLT model.[5] We suppose that this qualitative difference between the zero-temperature and nonzero-temperature M-H curves is due to the considerable difference in the dispersion curves of the low-lying excitations (''one-particle'' energy dispersion in the Bose-gas picture).[35,36] In the AKLT model, the one-particle dispersion curve $\omega(k)$ is flatter than that of the $\beta=0$ case, and $(k-\pi)^4$ and higher-order terms in $\omega(k)$ become significant. Accordingly, the δ-BG treatment will be valid only at very low temperature and at very low field.

For $\beta=0.6$ where the effective coupling $\tilde{c}$ is negative, agreement between the δ-BG curves and DMRG curves is even worse. This may be partly ascribed again to the shape of the one-particle dispersion curve, just as in the case of $\beta=1/3$. Further, as was briefly mentioned in the previous paper,[5] the zero-temperature M-H curve for $\beta>\beta_c$ (~ 0.41) shows a cusp singularity in the middle-field region which can never be explained in terms of a simple δ-BG picture. At finite temperatures, a remnant of the cusp singularity makes the M-H curve deviate significantly from the δ-BG curve. We should say that a naive δ-BG picture may not hold for $\beta>\beta_c$.

As has been pointed out in Refs. 36–39, the ground state and excitations for $\beta>\beta_c$ are quite different from those for $\beta<\beta_c$, which seems to be closely related to the inapplicability of the simple δ-BG treatment in this region.

VI. SUMMARY

We have investigated the M-H curve of the bilinear-biquadratic chain at finite temperatures by employing the density-matrix renormalization group to the quantum transfer matrices associated with Suzuki-Trotter-transformed 2D classical systems.

We have shown that the DMRG is an efficient tool to calculate the M-H curve, by verifying that it reproduces the exact curve of the $S=1/2$ XY model.

Based on the calculated curves, we have tested the δ-function Bose-gas picture for the BLBQ chain near the critical fields, varying the coefficient β of the biquadratic term.

Near the saturation field (upper critical field), we have mapped the BLBQ chain to the δ-BG through the exact two-body S matrices. The thermal Bethe-ansatz results of the correctly mapped δ-BG are consistent with the DMRG results. Further, we have extended the Bethe-ansatz approximation to finite-temperature, and have shown that the BAA gives better M-H curves than the δ-BG.

Near the lower critical field (associated with the Haldane gap), we have determined the parameters in the δ-BG Hamiltonian from the zero-temperature M-H curve, and have made thermal Bethe-ansatz calculation. At $\beta=0$ we have confirmed that the δ-BG gives consistent results with the DMRG calculations. On raising β, however, the δ-BG calculations deviate from the DMRG curves. One mechanism as for this discrepancy may be the nonparabolicity the excitation energy dispersion, which seems to explain the case for $\beta<\beta_c$ ($\beta_c \sim 0.41$). There seems to be another mechanism responsible for rather large deviation observed for $\beta>\beta_c$ (negative effective coupling region). The ground-state structure and property of low-lying excitations in this region may be qualitatively different from those in the region $\beta<\beta_c$.[36,39,40] The finite-temperature remnant of the middle-field cusp singularity at zero temperature also enhances the deviation. To clarify the formation mechanism of the cusp singularity itself is an interesting problem, which may also lead to a better understanding of the nature of the BLBQ chain in $\beta>\beta_c$. Details will be published elsewhere.[41]

ACKNOWLEDGMENTS

The author would like to thank Y. Akutsu, Y. Hieida, T. Nishino, H. Kiwata, and M. Kikuchi for fruitful discussions. The author is supported by JSPS.

[1] K. Katsumata, H. Hori, T. Takeuchi, M. Date, A. Yamagishi, and P.J. Renard, Phys. Rev. Lett. **63**, 86 (1989); Y. Ajiro, T. Goto, H. Kikuchi, T. Sakakibara, and T. Inami, *ibid.* **63**, 1424 (1989).
[2] M. Hagiwara, Y. Narumi, K. Kindo, M. Kohno, H. Nakano, R. Sato, and M. Takahashi, Phys. Rev. Lett. **80**, 1312 (1998).
[3] S. Yamamoto and S. Miyashita, Phys. Rev. B **51**, 3649 (1995).
[4] Y. Hieida, K. Okunishi, and Y. Akutsu, Phys. Lett. A **233**, 464 (1997).
[5] K. Okunishi, Y. Hieida, and Y. Akutsu, Phys. Rev. B **59**, 6806 (1999).
[6] S.R. White, Phys. Rev. Lett. **69**, 2863 (1992); Phys. Rev. B **48**, 10 345 (1993).
[7] X. Wang and T. Xiang, Phys. Rev. B **56**, 2221 (1997).
[8] N. Shibata, J. Phys. Soc. Jpn. **66**, 5061 (1997).
[9] T. Nishino, J. Phys. Soc. Jpn. **64**, 3598 (1995).
[10] H.A. Kramers and G.H. Wannier, Phys. Rev. **60**, 263 (1941).
[11] R.J. Baxter, J. Math. Phys. **9**, 650 (1968); J. Stat. Phys. **18**, 461 (1978).
[12] R.J. Baxter, *Exactly Solved Models in Statistical Mechanics* (Academic Press, London, 1982), p. 363.
[13] W. Krauth, Phys. Rev. B **44**, 9772 (1991).
[14] H. Kiwata and Y. Akutsu, J. Phys. Soc. Jpn. **63**, 3598 (1994).
[15] H. Betsuyaku and T. Yokota, Prog. Theor. Phys. **75**, 808 (1986).
[16] T. Nishino and K. Okunishi, J. Phys. Soc. Jpn. **64**, 4084 (1995).
[17] S.R. White, Phys. Rev. Lett. **77**, 3633 (1996).
[18] T. Nishino and K. Okunishi, J. Phys. Soc. Jpn. **65**, 891 (1996); **66**, 3040 (1997).
[19] S. Östlund and S. Rommer, Phys. Rev. Lett. **75**, 3537 (1995); S. Rommer and S. Östlund, Phys. Rev. B **55**, 2164 (1997).
[20] E. Lieb, T. Schultz, and D. Mattice, Ann. Phys. (N.Y.) **16**, 407 (1961).
[21] S. Katsura, Phys. Rev. **127**, 1508 (1962); **129**, 2835 (1963).
[22] I. Affleck, T. Kennedy, E.H. Lieb, and H. Tasaki, Phys. Rev. Lett. **59**, 799 (1987); Commun. Math. Phys. **115**, 477 (1988).
[23] M.D. Johnson and M. Fowler, Phys. Rev. B **34**, 1728 (1986).
[24] M. Takahashi and T. Sakai, J. Phys. Soc. Jpn. **60**, 760 (1991).
[25] R.P. Hodgeson and J.B. Parkinson, J. Phys. C **18**, 6385 (1985).
[26] E. Lieb and W. Liniger, Phys. Rev. **130**, 1605 (1963).
[27] C.N. Yang and C.P. Yang, J. Math. Phys. **10**, 1115 (1969).
[28] C.K. Lai, J. Math. Phys. **15**, 1675 (1974); B. Sutherland, Phys. Rev. B **12**, 3795 (1975).
[29] L.A. Takhtajan, Phys. Lett. **87A**, 479 (1982); H.M. Babujian, *ibid.* **90A**, 479 (1982).
[30] I. Affleck, Phys. Rev. B **43**, 3215 (1991).
[31] E. Sørensen and I. Affleck, Phys. Rev. Lett. **71**, 1633 (1993).
[32] D.P. Arovas, A. Auerbach, and F.D.M. Haldane, Phys. Rev. Lett. **60**, 531 (1988).
[33] G. Fáth and J. Sólyom, J. Phys.: Condens. Matter **5**, 8983 (1993).
[34] R. Scharf and H.-J. Mikeska, J. Phys.: Condens. Matter **7**, 5083 (1995).
[35] M. Takahashi, Phys. Rev. B **38**, 5188 (1988); Phys. Rev. Lett. **62**, 2313 (1989); Phys. Rev. B **50**, 3045 (1994).
[36] O. Golinelli, Th. Jolicoeur, and E. Sørensen, cond-mat/9812296.
[37] U. Schollwöck, Th. Joricoere, and T. Gael, Phys. Rev. B **53**, 3304 (1996).
[38] R.J. Bursill, T. Xiang, and G.A. Gehring, J. Phys. A **28**, 2109 (1995).
[39] S. Yamamoto, Int. J. Mod. Phys. B **12**, 1795 (1998).
[40] G. Fath and P.B. Littlewood, Phys. Rev. B **58**, R14 709 (1998).
[41] K. Okunishi, Y. Hieida, and Y. Akutsu, cond-mat/9904155.